Research Article

Muttaqin Hasan*, Muhammad Jamil, and Taufiq Saidi

Mechanical properties and durability of ultrahigh-performance concrete with calcined diatomaceous earth as cement replacement

https://doi.org/10.1515/jmbm-2022-0272 received August 22, 2022; accepted December 04, 2022

Abstract: Calcined diatomaceous earth (CDE) with a maximum grain size of 143 µm was used to partially replace 5 and 10% of cement in ultra-high-performance concrete (UHPC) mixtures. The other materials used in producing the concrete include Ordinary Portland Cement, iron ore powder, and river sand with maximum grain sizes 112.5, 231, and 766.2 µm, respectively. Moreover, the UHPC specimens designed with a water-cement ratio of 0.2 and a superplasticizer of 1.5% from the cement weight were tested for flow, compressive strength, flexural strength, splitting tensile strength, durability against NaCl and Na₂SO₄ attack, and resistance to 400, 500, and 600°C temperatures. The results showed that the use of 5 and 10% CDE to replace cement was able to increase the compressive strength, flexural strength, splitting tensile strength, the durability of UHPC against NaCl, and Na₂SO₄, as well as its resistance to high temperatures but reduced the mixture flow.

Keywords: ultra-high-performance concrete, calcined diatomaceous earth, strength

1 Introduction

Ultra-high-performance concrete (UHPC) is a relatively new construction material with very high strength developed in the 1990s in France [1–4]. It is possible to increase its compressive strength up to 800 MPa when

* Corresponding author: Muttaqin Hasan, Department of Civil Engineering, Universitas Syiah Kuala, Banda, Aceh, 23111, Indonesia, e-mail: muttaqin@unsyiah.ac.id Muhammad Jamil, Taufiq Saidi: Department of Civil Engineering, Universitas Syiah Kuala, Banda, Aceh, 23111, Indonesia

steel aggregates smaller than 800 µm are used with the addition of steel fiber under pressure and heat treatment curing [1]. UHPC also has excellent durability due to the reduced pore size and number [5–8] and has also been reported to have a very low absorption capacity and permeability [9–12], which makes it more resistant to freeze—thaw cycles [12–19] and chloride penetration [11,12,20]. This concrete is denser and has relatively homogeneous particle packing, which leads to a better fatigue performance and subsequently an increase in sustainable construction [21,22]. However, its reduced porosity makes it more susceptible to fire or elevated temperatures [23–26].

The production of UHPC requires a very large quantity of cement, which exceeds $1,000 \text{ kg/m}^3$ [27–29] or a combination of cement and silica fume with the silica fume quantity generally higher than 175 kg/m³ [27–43]. The large amount of cement consumed in UHPC production makes this concrete not an environmentally friendly construction material since cement has been reported to be one of the major contributors to the production of greenhouse gas emissions, especially CO₂ [44]. A total of 5-7% of global CO₂ emissions is caused by cement plants with each ton produced reported to be emitting 900 kg into the atmosphere [45]. The CO_2 emissions further lead to global warming and more disastrous consequences if not controlled and reduced [46,47]. To reduce using cement quantity in UHPC, many studies have been conducted to replace partially cement with mineral additives. Some of the additives usually added include fly ash [48,49], nano-silica [32,33], silica powder or silica flour [38,39], limestone powder [50-54], ground granulated blast furnace slag [43,54-57], quartz powder [51,57,58], rice husk ash [59], and glass powder [60,61]. Moreover, the production process requires using a special type of sand such as quartz [28,56] or silica sands [35-40,43]. It is also important to note that the curing process is also special as indicated by steam [2,34,38,58], moist [49,56], or heat treatment [5,13,18,28,29,35-39,55,35-40,62] curing. This means that it has a very high production cost and its application is limited [63,64].

Diatomaceous earth is classified as a natural class N pozzolanic material [65] and also as one of the supplementary cementing materials with relatively high silica content [66–68]. It is also possible to increase its silicate content through the calcination process. Several studies have been conducted to replace cement with this diatomaceous earth in high-strength concrete mixtures (concrete with a compressive strength between 45 and 90 MPa) [69–71] but none has focused on its use in UHPC mixtures (concrete with compressive strength above 90 MPa).

This study was used to design a mixture of UHPC using local materials such as river sand (RS), iron ore powder (IOP), Ordinary Portland Cement (OPC), and calcined diatomaceous earth (CDE). The quantity of cement used was not too high and partially replaced by CDE while the production was made through normal curing to ensure that the process is simpler and cost-friendly toward achieving wider application. In addition, the replacement of partial cement with CDE reduces negative environmental impact since CO₂ emitted is reduced by 78.48 tons for every 1,000 m³ of brick masonry work by using CDE as a 40% cement replacement in cement mortar production [72]. The aim of this study was, therefore, to determine the effect of partial replacement of OPC with CDE on flow, compressive strength, flexural strength, splitting tensile strength, durability against NaCl and Na2SO4 attack, and the resistance to high temperatures of UHPC.

2 Materials and methods

2.1 Materials

The materials used include OPC, calcined diatomite earth (CDE), IOP, and RS. The OPC was used as a binder while

CDE was used for partial replacement of cement. The IOP was used as filler while RS was used as aggregate. Meanwhile, the OPC used is a product of PT Solusi Bangun Andalas, which has a maximum grain size of 112.5 µm, while the CDE was produced from chunks of diatomaceous earth from Aceh Besar Regency by mashing and sieving to ensure that it passes through a #200 sieve, baked at 100°C for 24 h, and calcined in a laboratory furnace at 650°C for 5 h. The maximum diameter of the CDE particles used was 143 µm. Moreover, the IOP was produced from an iron ore mine located in Aceh Besar District through mashing and sieving to have a maximum diameter of 231 µm while the RS was also sieved to have a maximum diameter of 766.2 µm. The particle size distribution of OPC, CDE, IOP, and RS was analyzed through a particle size analyzer (PSA) test using a MicroBrook 2000 L PSA test device and the results are presented in Figure 1. Meanwhile, the specific surface and specific gravity of the four materials are shown in Table 1 while the chemical composition of OPC and CDE determined using the X-ray fluorescence test is indicated in Table 2. The clean water supplied by PDAM (Local Water Company) was used for mixing while a polycarboxylate-based superplasticizer with a specific gravity of 1.06 was applied to adjust the concrete workability.

2.2 Mix proportion

The mix proportion of the solid materials in the UHPC was determined using the Modified Andreasen and Andersen Model (MAAM), which involved producing a target curve for the volume of the solid material distributed in the concrete using the following equation [73–78]:

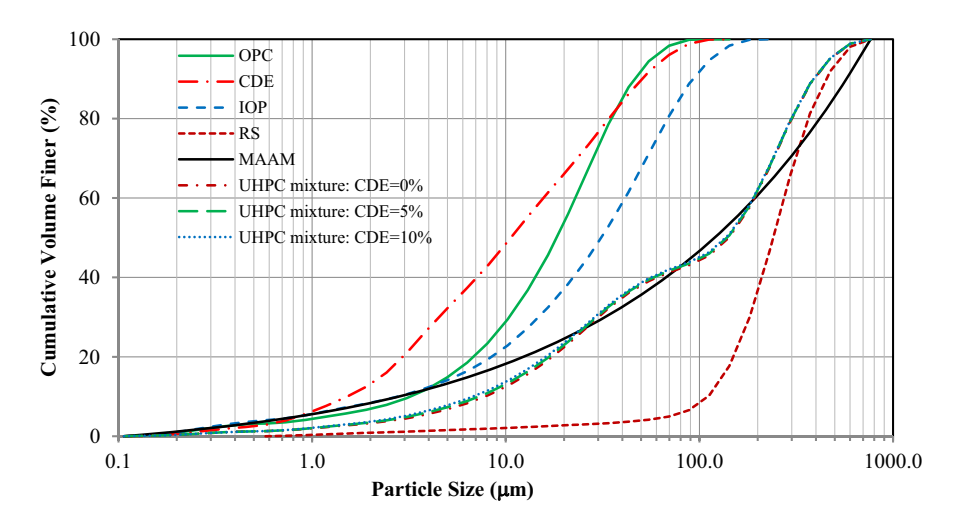


Figure 1: Particle size distribution of materials, target curve (MAAM), and grading curve of UHPC mixtures.

Table 1: Specific surface and specific gravity of materials

| Materials | Specific surface (m ² /kg) | Specific gravity |
|-----------|---------------------------------------|------------------|
| ОРС | 539.80 | 3.16 |
| CDE | 675.60 | 2.18 |
| IOP | 574.20 | 3.57 |
| RS | 370.00 | 2.65 |

Table 2: Chemical composition of OPC and CDE

| Chemical analysis | OPC (%) | CDE (%) |
|-------------------|---------|---------|
| CaO | 70.34 | 16.34 |
| SiO ₂ | 17.25 | 78.73 |
| Al_2O_3 | 2.32 | 0.39 |
| Fe_2O_3 | 4.67 | 2.89 |
| MgO | 2.13 | 1.11 |
| SO ₃ | 2.56 | 0.39 |
| K ₂ O | 0.73 | 0.15 |

$$P(D) = \frac{D^q - D_{\min}^q}{D_{\max}^q - D_{\min}^q},$$
 (1)

where P(D) is the volume fraction of solid materials with sizes smaller than D, D is the solid material particle size, D_{\min} is the minimum particle size, D_{\max} is the maximum particle size, and q is the modulus distribution. A software known as EMMA from Elkem was used to simplify the mix design process and speed up the packing density calculation process. Moreover, a q value, which is less than 0.36, is required for optimal packing density while a value of higher than 0.25 is needed for a good flow [79]. Therefore, this study set the q value at 0.35.

The proportion of each solid material in the mixture was adjusted to ensure an optimal match between the prepared mixture and the target curve. The reduction in the deviation between the target curve and the mixture made it possible to use the concrete composition. An optimum comparison was achieved by minimizing the sum of the residual squares as follows [74,75]:

RSS =
$$\sum_{i=1}^{n} (P_{\text{mix}}(D_i^{i+1}) - P_{\text{tar}}(D_i^{i+1}))^2$$
, (2)

where RSS is the sum of the residual squares, $P_{\rm mix}$ is the mixture gradation, and P_{tar} is the target grading according to MAAM.

The proportion of mixtures without CDE was first determined and this includes the solid materials consisting of the OPC, IOP, and RS. This was followed by the replacement of 5 and 10% of the OPC with CDE in other mixtures. This means that three UHPC mixes were used in this study and their grading curves presented in Figure 1

are observed to be very close to the target curve. Moreover, the quantity of water used was determined based on the water-cement ratio (w/c) of 0.2 while the superplasticizer was set at 1.5% of the cement weight. The mix proportions of the three UHPC mixtures is presented in Table 3.

2.3 Preparation of specimens

The UHPC specimens were produced by mixing all the materials in a mixer using the procedure suggested by Yu et al. [74]. This involved placing all the solid materials including OPC, CDE, IOP, and RS in a mixer and stirred at low speed for 30 s as indicated in Figure 2. The process was followed by the addition of 80% of the mixing water to the mixer and stirred at low speed for 90 s after which it was stopped for 30 s. Finally, the remaining mixing water and superplasticizer were added and stirred at low speed for 180 s and later at high speed for 120 s.

The UHPC mixtures were cast into steel molds and each mixture has 85 cube specimens with 75 mm size, 10 beam specimens with $75 \,\mathrm{m} \times 75 \,\mathrm{mm} \times 350 \,\mathrm{mm}$ dimension, and 10 cylinder specimens with 50 mm diameter and 100 mm height. The cube specimens were used for the compression test, exposure to NaCl and Na2SO4, and exposure to high temperatures. The beam specimens were used for four points bending test while the cylinder specimens were for the split tensile test. The specimen' shape and size used in this study were based on previous studies [48,80,81]. It is important to note that five specimens were used for each test. Moreover, the molds were removed after 24 h of casting and cured in fresh water for 28 days.

2.4 Flow test

The flow tests were conducted based on the procedure in ASTM C 1437-07 [82] using the apparatus described in

Table 3: Mix proportion for 1 m³ concrete volume

| Materials | Weight (kg) | | |
|-----------------------|-------------|---------|---------|
| Replacement level (%) | 0 | 5 | 10 |
| OPC | 872.00 | 828.40 | 784.80 |
| CDE | 0.00 | 43.60 | 87.20 |
| IOP | 87.20 | 87.20 | 87.20 |
| RS | 1220.80 | 1220.80 | 1220.80 |
| Water | 174.40 | 174.40 | 174.40 |
| Superplasticizer | 13.08 | 13.08 | 13.08 |



Figure 2: Mixing of UHPC mixture.

ASTM C 230/C 230M-08 [83]. This involved placing steel cones designed with a bottom and top diameter of 4, 2.75, and 2 in. height at the middle of the flow table. The freshly mixed concrete was then placed into the steel cone in two layers. Each layer was tamped 20 times. Moreover, the surface of the concrete mixture at the top of the cone was leveled after which the cone was lifted for the concrete mixture to flow around and the flow table was immediately vibrated 25 times in 15 s. The flow diameter of the concrete mixture was measured four times at different positions and the average value was recorded as indicated in Figure 3. The flow value was, therefore, calculated in percentage using the following equation:

$$F_{\nu} = \frac{D_{\text{avg}} - D_{\text{o}}}{D_{\text{o}}} \times 100\%,$$
 (3)

where F_{ν} is the flow value, $D_{\rm avg}$ is the average flow diameter, and $D_{\rm o}$ is the inner diameter on the bottom of the steel cone.



Figure 3: Flow test.



Figure 4: Compression test.

2.5 Mechanical properties test

The mechanical properties of the UHPC were tested when the specimens were 7 and 28 days old. The process involved removing the specimens from the bath and wiped with a cloth to dry a day before the test. The compressive strength was determined by placing the specimen between two plates of the compression test machine and a compressive load was applied up to the moment the specimen was failed as shown in Figure 4. The flexural strength was evaluated using the four-point bending test and this involved subjecting a beam placed on two supports at a span of 300 mm to two equal loads, which are at 75 mm from each support up to the period the specimen was crushed as shown in Figure 5. Meanwhile, the splitting tensile strength test was conducted by laying down the cylinder specimens on the plate of the testing machine and a load was applied from



Figure 5: Four-point bending test.



Figure 6: Splitting tensile test.

the top up to the moment the specimen was crushed as shown in Figure 6.



Figure 7: The specimens exposed to NaCl and Na₂SO₄ solution.

used for each mixture with five specimens removed after 1, 2, 5, 7, 9, and 12 months of immersion for visual observation, mass weighing, and compressive strength test.

2.6 Exposure to NaCl and Na₂SO₄ solutions

The UHPC specimens were exposed to NaCl and Na₂SO₄ to determine their durability against the attack of these chemicals. The test was conducted separately on 28-dayold cube specimens. The specimens used were removed from the water curing the day before the test, wiped till they dry, and left at room temperature for 24 h. Moreover, the specimens were weighed before exposure to determine their mass using a digital scale and also tested for compressive strength. The process involved immersing the specimens separately in 10% NaCl and 10% Na₂SO₄ solutions, respectively, as shown in Figure 7 with the vessel being in a closed state during the process. It is important to note that a total of 30 cube specimens were

2.7 Exposure to high temperatures

The specimens were also exposed to high temperatures to determine the resistance of UHPC to heat. The test was also conducted after the specimens were 28 days old. The specimens used were removed from the water curing the day before the test, wiped till they dry, and left at room temperature for 24 h. Their mass and compressive strength were also determined after which they were inserted into a laboratory furnace as shown in Figure 8 and exposed to temperatures of 400, 500, and 600°C for 5h, respectively. This was followed by the removal of each of the specimens from the furnace and allowed to room temperature for visual observation, mass weighing, and compressive strength test.





Figure 8: The exposure of the specimens in the laboratory furnace: (a) temperature set up and (b) specimens in the furnace.

3 Results and discussion

3.1 Flow of UHPC

Figure 9 shows that the UHPC flow value decreased as the CDE increased but all the UHPC mixtures flow easily and compact when cast in the molds. The decrease in the flow value was associated with the water-absorbing characteristics of the CDE used to replace cement as well as the fact that the more quantity of finer particles of CDE needed a higher quantity of water to become wet when compared to the cement surface. This result was found to be in line with the findings of several previous studies [68,84].

3.2 Mechanical properties of UHPC

The mechanical properties of the UHPC including compressive, flexural, and splitting tensile strengths were tested at the age of 7 and 28 days and the results are presented in Figures 10-12. It was discovered that the use of CDE as a cement replacement at 5 and 10% levels was able to increase the strength of UHPC with the highest recorded at 10%. This was associated with the more quantity of finer particles in CDE compared to the OPC, which produced more cavities to be filled, thereby making the UHPC denser with higher strength. It was also related to the occurrence of a second reaction between silica in CDE and calcium hydroxide from the cement hydration to form calcium silicate hydrate, which also makes UHPC denser [76], thereby increasing its strength. However, this second reaction occurred at a longer age; therefore, the compressive strength of the mixture at 7 days of age was observed to be lower than the UHPC without CDE as shown in Figure 10.

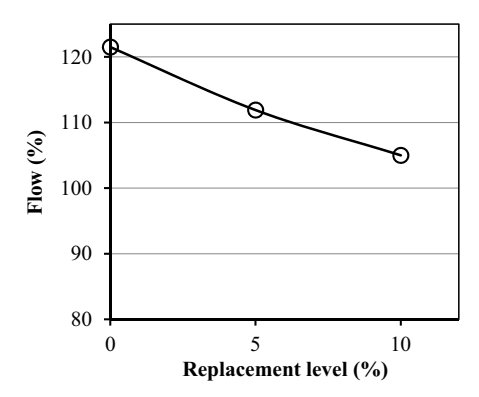


Figure 9: Flow of UHPC.

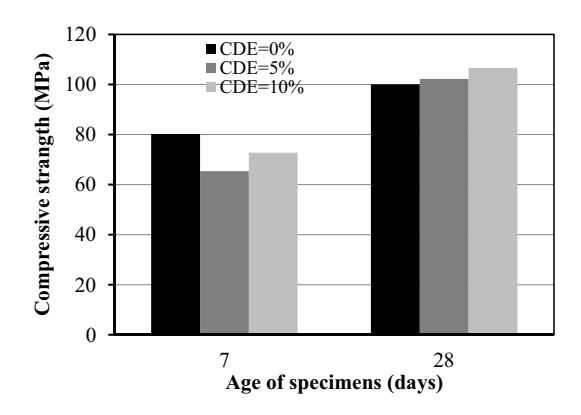


Figure 10: Compressive strength of UHPC.

3.3 The resistance of UHPC to NaCl and Na_2SO_4

The chemical attack of sulfates on concrete structures has the ability to degrade the quality of concrete exposed to sulfate-rich environments. Moreover, the damage of concrete caused by sulfate is due to the combination of physical and chemical attacks [85,86]. The physical attack mainly induces surface scaling of the aboveground concrete while the chemical attack generally involves chemical interactions between sulfate ions and cement paste components, thereby leading to the loss of adhesion for the cement hydration products and the formation of ettringite, gypsum, and/or softening due to thaumasite formation [86]. In contrast to the complex chemistry of the sulfate attack process, chloride ion penetration is more physical through ionic bonding and reduction, which has the ability to reach the reinforcing steel if not eliminated [87]. It is important to note that the attacks caused by sulfate and chloride reduce the compressive strength of concrete. This study, therefore, examined the durability of the UHPC produced by partially replacing

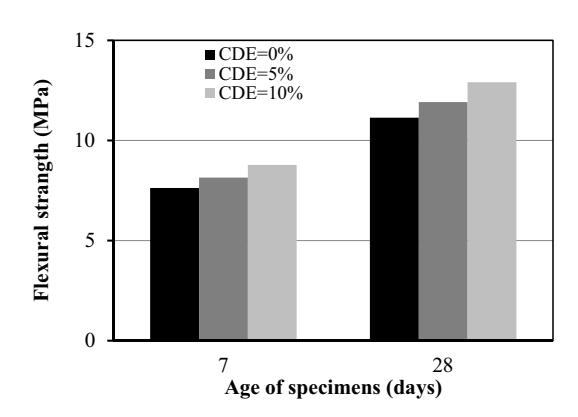


Figure 11: Flexural strength of UHPC.

Figure 12: Splitting tensile strength of UHPC.

DE GRUYTER

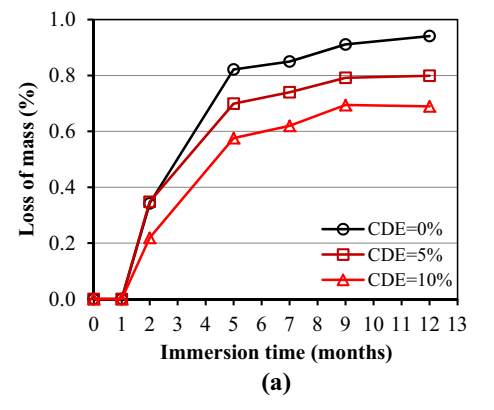
cement with CDE through the measurement of the mass loss and changes in compressive strength after the specimens were immersed in 10% NaCl and 10% Na₂SO₄ solutions.

The result for the mass loss after 12 months of immersion is presented in Figure 13a and b and it was discovered that the specimen under NaCl attack only showed mass loss after 2 months of immersion while the Na₂SO₄ attack caused an immediate mass loss after 1 month of immersion. The mechanism of chloride attack on concrete started with the penetration of chloride ions into concrete pore structures in the first month of immersion. During this process, the surface scaling was not induced therefore the concrete mass remained constant. No mass loss could be observed during this period as presented in Figure 13a. After the chloride ion penetrated the pore structures of concrete, the chemical reaction between chloride ion and cement-based materials is happened to produce calcium oxychloride [88]. The presence of calcium oxychloride makes concrete damage in the form of surface scaling and more internal cracking. The surface scaling reduces the mass of concrete as shown in Figure 13a after

the immersion time of 2 months and more. The figures also showed that the mass lost by the UHPC with CDE is smaller than the value recorded by UHPC without CDE and the specimen with 10% replacement had the least loss. The lower mass loss of UHPC with 5% CDE compared to that of UHPC with 10% CDE at 1 month immersion time shown in Figure 13b was due to the variation in the mass loss data of UHPC with 5% CDE where two of the data have a very small mass loss, which results in the lower average value.

The compressive strength of the UHPC before and after 1, 2, 5, 7, 9, and 12 months of being exposed to NaCl and Na₂SO₄ solutions are presented in Figure 14a and b. The compressive strength ratio after exposure (f'_{ci}) and before exposure (f'_{co}) was plotted as a function of the immersion time in Figure 15 to determine the compressive strength degradation due to the impact of the exposures. The results showed that the compressive strength degradation of the UHPC with CDE was lower than the value for the UHPC without CDE and this means that the presence of CDE in UHPC was able to increase the resistance of the concrete to NaCl and Na₂SO₄ attacks. The effectiveness of pozzolan materials in increasing the durability of concrete against chloride and sulfate attacks has also been reported in several previous studies [89,90].

Figure 16 compares the mass loss and compressive strength degradation of UHPC with different CDE replacement levels due to NaCl and Na2SO4 attacks and the mass loss of all the UHPC mixture due to Na2SO4 attacks that was found to be greater than those for NaCl attacks starting from the beginning to the 12 months of soaking. Meanwhile, the compressive strength degradation due to NaCl attacks and Na₂SO₄ attacks was observed to be almost the same up to 9 months while NaCl was discovered to have a greater impact after 12 months of exposure. This shows that the reduction in concrete compressive strength due to chloride and sulfate salt attacks has no



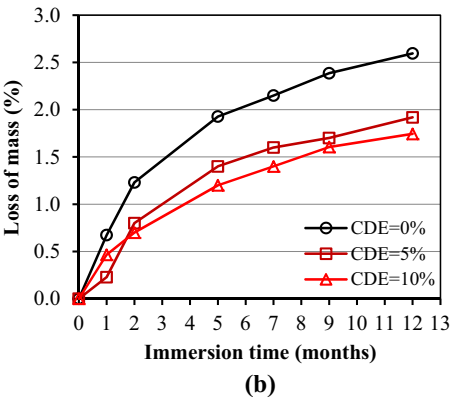


Figure 13: Loss of mass of UHPC after being immersed in: (a) NaCl and (b) Na2SO4 solutions.

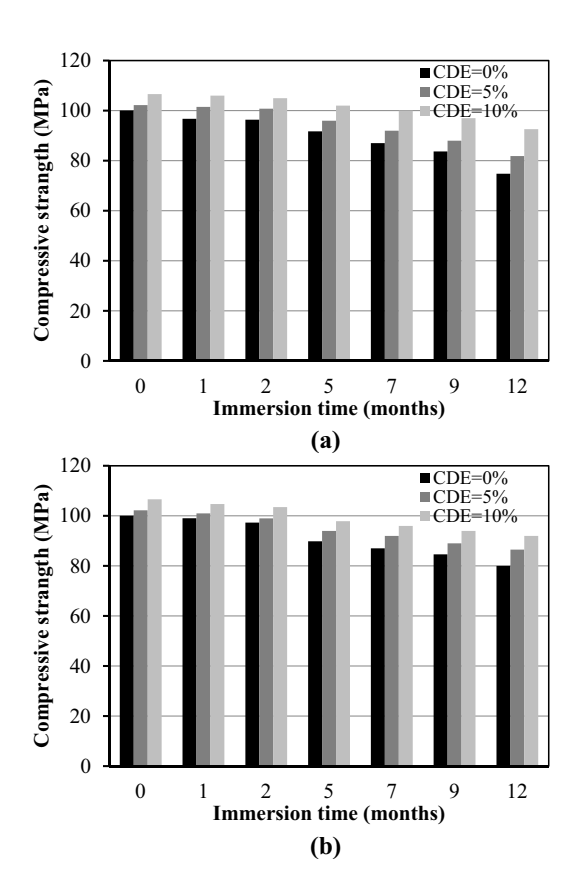


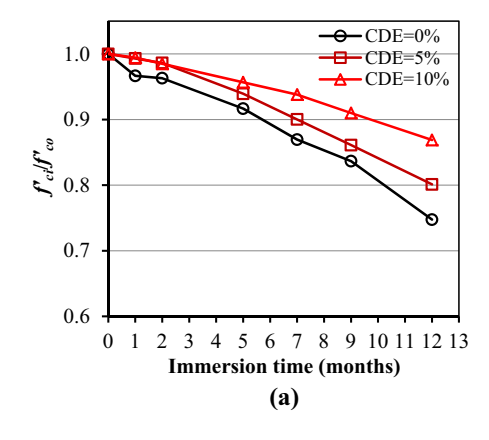
Figure 14: Compressive strength of UHPC after being immersed in: (a) NaCl and (b) Na_2SO_4 solutions.

direct relationship with the loss of its mass. It was, however, discovered that the mass loss was due to the occurrence of surface scaling with the Na_2SO_4 attack observed to be higher than NaCl attack while compressive strength degradation was due to internal cracking.

The mass loss of concrete under sulfate and chloride attack is associated with the surface scaling of concrete. In real concrete structures, surface scaling reduces the section area of the structures, which results in the degradation of load-carrying capacity. Furthermore, the internal cracking of concrete in the sulfate- and chloride-rich environment causes the degradation of the compressive strength and tensile strength of concrete. The lower compressive and tensile strength and the propagation of cracks may cause the structures to collapse in their service life. The use of 10% CDE as cement replacement in the UHPC mixture tested in this study showed lower mass loss and compressive strength degradation. These results indicated that the replacement of 10% cement weight with CDE in a UHPC mixture improves the resistance of UHPC to the sulfate- and chloride-rich environments with less surface scaling and internal cracking. Therefore, concrete structures containing CDE as cement replacement at a 10% replacement level have better long-life performance and service life in an environment with rich sulfate and chloride ions.

3.4 The resistance of UHPC to high temperatures

Figure 17 shows the mass loss for the UHPC after exposure to 400, 500, and 600°C temperature, and the mass loss was found to be increasing as the temperature increased. This was associated with the vaporization of the evaporable water and a part of the bound water in the concrete by the high temperature [25]. Figure 17 also indicates that the mass loss by the UHPC with CDE was lower than for UHPC without CDE with the lowest value recorded in the specimen with 5% replacement. It is important to note that the UHPC with CDE has a denser mass with fewer cavities, thereby making its water content to be smaller, and this led to the loss of a lesser quantity of mass after exposure to high temperatures.



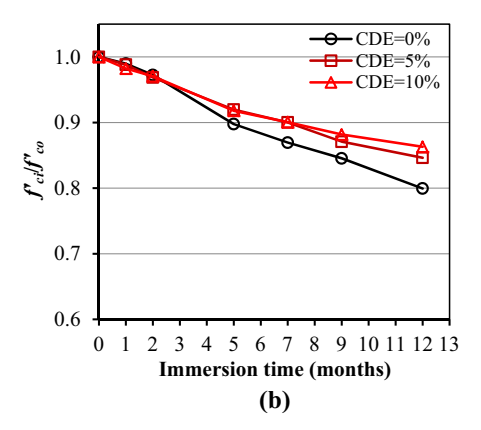


Figure 15: Degradation of compressive strength due to (a) NaCl and (b) Na₂SO₄ exposures.

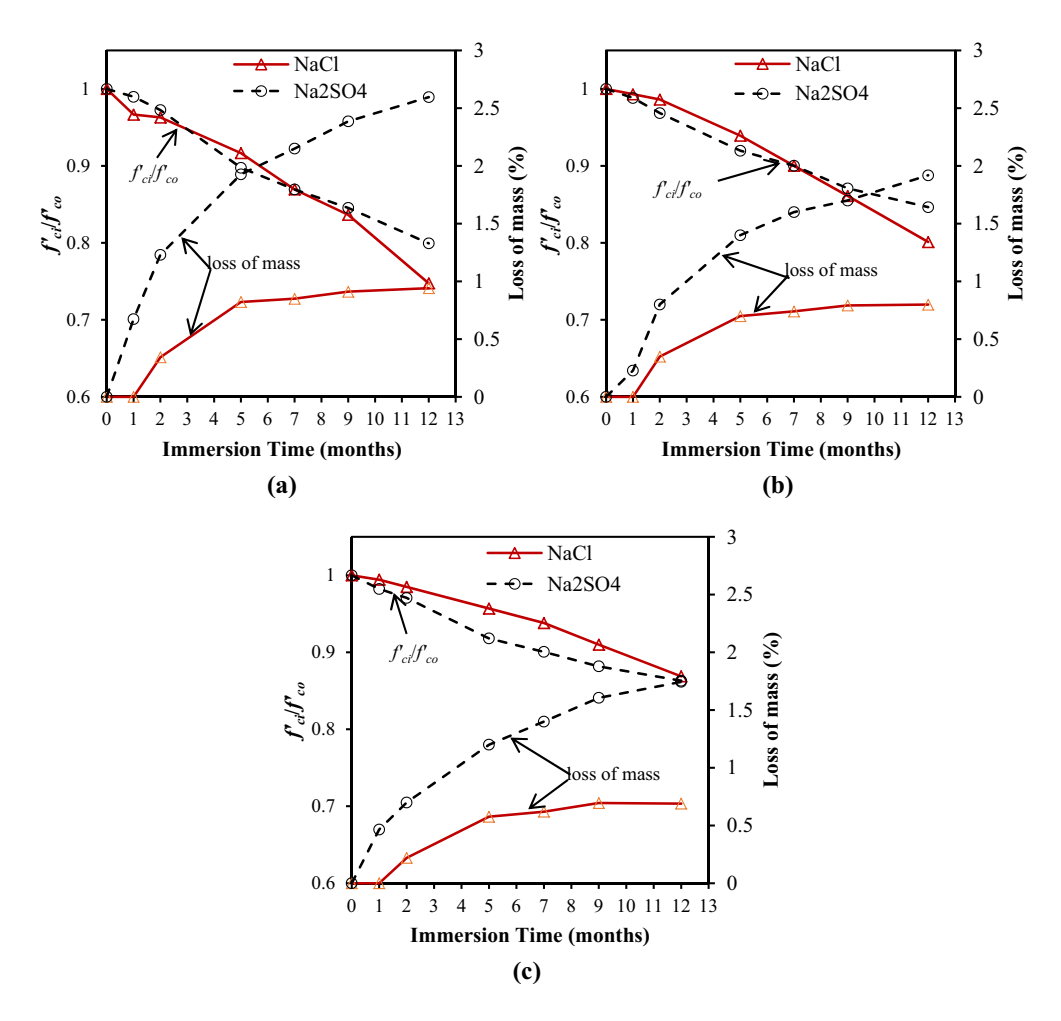


Figure 16: Comparison of mass loss and compressive strength degradation of UHPC with CDE at (a) 0%; (b) 5%; and (c) 10% after exposure to NaCl and Na₂SO₄ solutions.

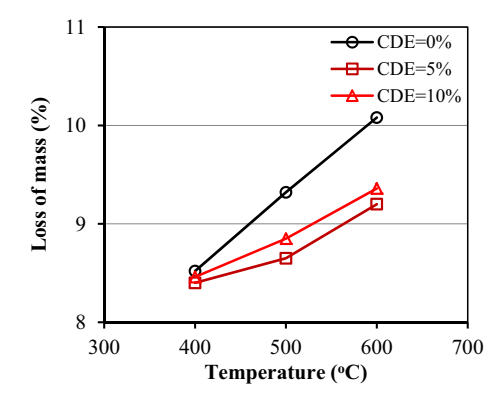


Figure 17: Mass loss of UHPC after being exposed to high temperatures.

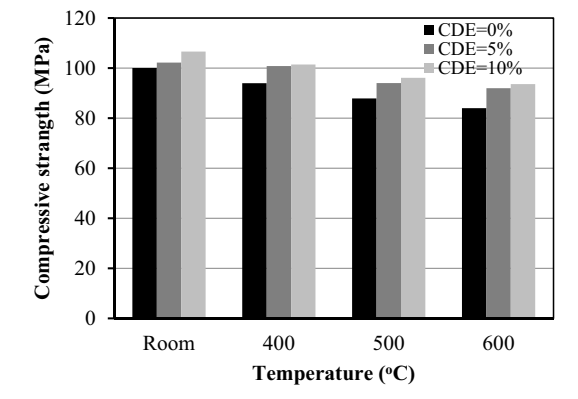


Figure 18: Compressive strength of UHPC after being exposed to high temperatures.

Figure 18 shows the compressive strength of UHPC before and after being exposed to 400, 500, and 600°C temperature, and the compressive strength was observed to be decreasing with the high temperatures. Moreover,

the degradation graph of the compressive strength after being exposed ($f'_{\rm CT}$) and before being exposed ($f'_{\rm co}$) to high temperatures was plotted as a function of the temperature in Figure 19 to determine the resilience of all the

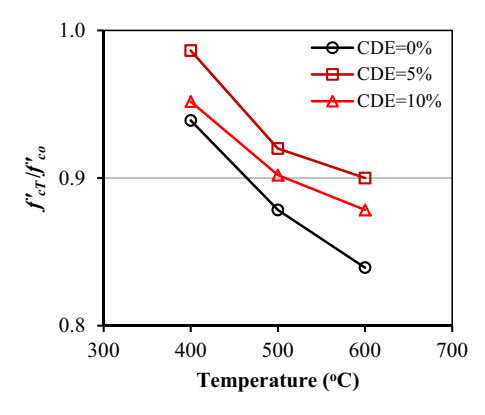


Figure 19: Degradation of compressive strength due to high-temperature exposures.

mixes tested. The results showed that the use of CDE for the partial replacement of cement was able to increase the resistance of UHPC to high temperatures with the best resilience obtained at 5% replacement. Meanwhile, the compressive strength degradation recorded in this study is smaller than that recorded in some of the previous studies [25,91].

4 Conclusions

UHPC specimens were produced by replacing 5 and 10% of cement with CDE after which the flow, strengths, and durability of the specimens against NaCl and Na₂SO₄ attacks and high temperatures were tested. The results showed that the use of CDE as a replacement of 5 and 10% cement in the UHPC mixture was able to increase strength, durability against NaCl and Na₂SO₄ attacks, and high-temperature resistance of the concrete. This is further explained as follows:

- 1. The use of CDE to partially replace 5 and 10% cement in the UHPC mixture increased the compressive, flexural, and splitting tensile strengths of the UHPC and the highest strength was achieved in the mixture with a 10% replacement.
- 2. The flow from the UHPC was reduced due to the increasing use of CDE as a replacement for cement but the specimen with 10% replacement was observed to flow easily during casting.
- 3. The use of CDE to partially replace 5 and 10% cement in the UHPC mixture was also able to increase UHPC durability against NaCl and Na_2SO_4 attacks. The mass loss and compressive strength degradation were discovered to be increasing as the exposure time increased. The UHPC mass loss under the Na_2SO_4 attack was also

found to be higher than NaCl, but the strength degradation was the same except after 12 months when NaCl had higher degradation. The best durability was, however, obtained with 10% replacement.

4. The use of CDE to partially replace 5 and 10% cement in the UHPC mixture also increased the UHPC resistance to 400, 500, and 600°C temperature. The mass loss and compressive strength degradation were observed to increase as the exposure to temperature increased but the best resilience was recorded with the 5% replacement.

Acknowledgments: This research was supported by a grant provided by the Directorate of Research and Community Service, Ministry of Research and Technology/National Research and Innovation Agency, Republic of Indonesia (contract number: 154/SP2H/LT/DPRM/2021) and Research and Community Service Center of Syiah Kuala University (contract number: 28/UN/11.2.1/PT.01.03/DPRM/2021). The authors are grateful to Mr. Azzaki Mubarak, Mr. Mahlil, and Mr. Razali for their assistance with the experimental work.

Funding information: This research was funded by the Directorate of Research and Community Service, Ministry of Research and Technology/National Research and Innovation Agency, Republic of Indonesia (contract number: 154/SP2H/LT/DPRM/2021)

Author contributions: All authors have accepted responsibility for the entire content of this manuscript and approved its submission.

Conflict of interest: Authors state no conflict of interest.

References

- Richard P, Cheyrezy M. Composition of reactive powder concretes. Cem Concr Res. 1995;25:1501–11.
- [2] Aldahdooh MAA, Bunnori NM, Johari NAM. Evaluation of ultra-high performance-fiber reinforced concrete binder content using the response surface method. Mater Des. 2013;52:957–65.
- [3] Ghafari E, Costa H, Júlio E, Portugal A, Durães L. The effect of nanosilica addition on flowability, strength and transport properties of ultra-high performance concrete. Mater Des. 2014;59:1–9.
- [4] Akhnoukh AK, Buckhalter C. Ultra-high-performance concrete: Constituents, mechanical properties, applications and current challenges. Case Stud Constr Mater. 2021;15:e00559.
- [5] Heinz D, Ludwig H. Heat treatment and the risk of DEF delayed ettringite formation in UHPC. In: Schmidt M, Fehling E, Geisenhanslüke C, editors. Proceedings of the International

- Symposium on Ultra-High Performance Concrete; 2004 Sep 13-15; Kassel, Germany. Kassel University Press, 2004. p. 717-30.
- Herold G, Muller H. Measurement of porosity of ultra-high strength fibre reinforced concrete. In: Schmidt M, Fehling E, Geisenhanslüke C, editors. Proceedings of the International Symposium on Ultra-High Performance Concrete; 2004 Sep 13-15; Kassel, Germany. Kassel University Press, 2004. p. 685-94.
- El-Dieb AS. Mechanical, durability and microstructural characteristics of ultra-high-strength self-compacting concrete incorporating steel fibers. Mater Des. 2009;30:4286-92.
- Tuan NV, Ye G, van Breugel K, Copuroglu O. Hydration and microstructure of ultra high performance concrete incorporating rice husk ash. Cem Concr Res. 2011:41:1104-11.
- Schmidt M, Fehling E. Ultra-high-performance concrete: research, development and application in Europe. In: Russel HG, editor. Proceedings of the 7th International Symposium on the Utilization of High-Strength/High-Performance Concrete; 2005 Jun 20-24; Washington D.C., USA. ACI, 2005. p. 51-77.
- [10] Pierard J, Cauberg N. Evaluation of durability and cracking tendency of ultra-high performance concrete. Creep, shrinkage and durability mechanics of concrete and concrete structures. London, UK: Taylor and Francis Group; 2009. p. 695-700.
- [11] Tayeh BA, Bakar BHA, Johari MAM, Voo YL. Mechanical and permeability properties of the interface between normal concrete substrate and ultra high performance fiber concrete overlay. Constr Build Mater. 2012;36:538-48.
- [12] Alkaysi M, El-Tawil S, Liu Z, Hansen W. Effects of silica powder and cement type on durability of ultra high performance concrete (UHPC). Cem Concr Compos. 2016;66:47-56.
- [13] Graybeal B. Material property characterization of ultrahigh performance concrete, FHWA-HRT-06-103. U.S. Department of Transportation; 2006. p. 176.
- [14] Bonneau O, Vernet C, Moranville M, Aitcin P. Characterization of the granular packing and percolation threshold of reactive powder concrete. Cem Concr Res. 2000;30:1861-7.
- Bonneau O, Lachemi M, Dallaire E, Dugat J, Aitcin P. Mechanical properties and durability of two industrial reactive powder concretes. ACI Mater J. 1997;94:286-90.
- [16] Juanhong L, Shaomin S, Lin W. Durability and micro-structure of reactive powder concrete. J Wuhan Univ Technol Mater. 2009;24:506-9.
- [17] Vernet P. Ultra-durable concretes: Structure at the micro- and nano-scale. Mater Res Soc. 2004;29:324-7.
- [18] Cwirzen A, Penttala V, Cwirzen K. The effect of heat treatment on the salt freeze-thaw durability of UHSC. In: Fehling E, Schmidt M, Stürwald S, editors. Proceedings of 2nd International Symposium on Ultra-High Performance Concrete; 2008 Mar 5-7; Kassel, Germany. Kassel University Press, 2004. p. 685-94.
- [19] Shaheen E, Shrive N. Optimization of mechanical properties and durability of reactive powder concrete. ACI Mater J. 2006;103:444-51.
- [20] Gao R, Liu Z, Zhang L, Stroeven P. Static properties of reactive powder concrete beams. Key Eng Mater. 2006;302:521-7.
- [21] Abbas S, Nehdi ML, Saleem MA. Ultra-high performance concrete: Mechanical performance, durability, sustainability and implementation challenges. Int J Concr Struct Mater. 2016;10:271-95.

- [22] Brühwiler E, Denarié E. Rehabilitation and strengthening of concrete structures using ultra-high performance fibre reinforced concrete. Struct Eng Int. 2013;4:450-7.
- [23] Way R, Wille K. Material characterization of an ultra-high performance fibre-reinforced concrete under elevated temperature. In: Schmidt M, editor. Proceedings of 2nd International Symposium on Ultra-High Performance Concrete; 2012 Mar 7-9; Kassel, Germany. Kassel University Press, 2012. p. 565-72.
- Pimienta P, Mindeguia J, Simon A, Behloul M, Felicetti R, Bamonte P, et al. Literature review on the behaviour of UHPFRC at high temperature. In: Schmidt M, editor. Proceedings of 2nd International Symposium on Ultra-High Performance Concrete; 2012 Mar 7-9; Kassel, Germany. Kassel University Press, 2012. p. 549-56.
- [25] Tai S, Pan H, Kung N. Mechanical properties of steel fiber reinforced reactive powder concrete following exposure to high temperature reaching 800 C. Nucl Eng Des. 2011;241:2416-24.
- [26] Zhu Y, Hussein H, Kumar A, Chen G. A review: Material and structural properties of UHPC at elevated temperatures or fire conditions. Cem Concr Compos. 2021;123:104212.
- [27] Toledo Filho RD, Koenders EAB, Formagini S, Fairbairn EMR. Performance assessment of ultra high performance fiber reinforced cementitious composites in view of sustainability. Mater Des. 2021;36:880-8.
- Habel K, Viviani M, Denarié E, Brühwiler E. Development of the mechanical properties of an ultra-high performance fiber reinforced concrete (UHPFRC). Cem Concr Res. 2006;26:1362-70.
- [29] Rossi P. Influence of fibre geometry and matrix maturity on the mechanical performance of ultra high-performance cementbased composites. Cem Concr Compos. 2013;37:246-8.
- [30] Aldahdooh MAA, Bunnori NM, Johari MAM. Evaluation of ultra-high-performance-fiber reinforced concrete binder content using the response surface method. Mater Des. 2013:52:957-65.
- [31] Corinaldesi V, Moriconi G. Mechanical and thermal evaluation of ultra high performance fiber reinforced concretes for engineering applications. Constr Build Mater. 2012;26:289-94.
- Ghafari E, Costa H, Júlio E, Portugal A, Durães L. The effect [32] of nanosilica addition on flowability, strength and transport properties of ultra high performance concrete. Mater Des. 2014;59:1-9.
- [33] Ghafari E, Arezoumandi M, Costa H, Júlio E. Influence of nano-silica addition in the durability of UHPC. Constr Build Mater. 2015;95:181-8.
- [34] Huang H, Gao X, Khayat KH. Contribution of fiber alignment on flexural properties of UHPC and prediction using the composite theory. Cem Concr Compos. 2021;118:103971.
- [35] Yoo DY, Shin W. Improvement of fiber corrosion resistance of ultra-high-performance concrete by means of crack width control and repair. Cem Concr Compos. 2021;121:104073.
- Yoo DY, Jang YS, Chun B, Kim S. Chelate effect on fiber surface morphology and its benefits on pullout and split tensile behaviors of ultra-high-performance concrete. Cem Concr Compos. 2021;115:103864.
- Yoo DY, Shin W, Chun B. Corrosion effect on tensile behavior of [37] ultra-high-performance concrete reinforced with straight steel fibers. Cem Concr Compos. 2020;109:103566.
- [38] Kim JJ, Yoo YY. Effects of fiber shape and distance on the pullout behavior of steel fibers embedded in ultra-high-performance concrete. Cem Concr Compos. 2019;103:213-23.

- [39] Le HV, Kim MK, Kim DJ, Park J. Electrical properties of smart ultrahigh performance concrete under various temperatures, humidities, and age of concrete. Cem Concr Compos. 2021;118:103979.
- [40] Zhang D, Tan KH, Dasari A, Weng Y. Effect of natural fibers on thermal spalling resistance of ultra-high performance concrete. Cem Concr Compos. 2020;109:103512.
- [41] Wu Z, Shi C, Khayat KH. Multi-scale investigation of microstructure, fiber pullout behavior, and mechanical properties of ultra-high performance concrete with nano CaCO3 particle. Cem Concr Compos. 2018;86:255-65.
- [42] Tuan NV, Ye G, van Breugel K, Fraaij ALA, Dai BD. The study of using rice husk ash to produce ultra high performance concrete. Const Build Mater. 2011;25:2030-5.
- [43] Yua KQ, Dai JG, Luc ZD, Poon CS. Rate-dependent tensile properties of ultra-high performance engineered cementitious composites (UHP-ECC). Cem Concr Compos. 2018;93:218–34.
- [44] Hanle L, Maldonado P, Onuma E, Tichy M, Van Oss GH. IPCC guideline for national greenhouse gas inventories, Chapter 2: Mineral industry emission. Hayana, Kanagawa, Japan: IGES; 2006.
- [45] Benhelal E, Zahedi G, Shamsaei E, Bahadori A. Global strategies and potentials to curb ${\rm CO_2}$ emission in cement industry. J Clean Prod. 2013;51:142-61.
- [46] Mahlia TMI. Emission from electricity generation in Malaysia. Renew. Energy. 2002;27:293–300.
- [47] Zhang XF, Zhang SY, Hu ZY, Yu G, Pei CH, Sa RN. Identification of connection units with high GHC emissions for low-carbon product structure design. J Clean Prod. 2012;27:118–25.
- [48] Teng L, Huang H, Du J, Khayat KH. Prediction of fiber orientation and flexural performance of UHPC based on suspending mortar rheology and casting method. Cem Concr Compos. 2021;122:104142.
- [49] Mobasher B, Li A, Yao Y, Arora A, Neithalath N. Characterization of toughening mechanisms in UHPC through image correlation and inverse analysis of flexural results. Cem Concr Compos. 2021;122:104157.
- [50] Habert G, Denarié E, Šajna A, Rossi P. Lowering the global warming impact of bridge rehabilitations by using ultra high performance fibre reinforced concretes. Cem Concr Compos. 2013;38:1–11.
- [51] Yu R, Spiesz P, Brouwers HJH. Effect of nano-silica on the hydration and microstructure development of Ultra-High Performance Concrete (UHPC) with a low binder amount. Constr Build Mater. 2014;65:140–50.
- [52] Yu R, Spiesz P, Brouwers HJH. Static properties and impact resistance of a green ultra-high performance hybrid fibre reinforced concrete (UHPHFRC): Experiments and modeling. Constr Build Mater. 2014;68:158–71.
- [53] Yu R, Tang P, Spiesz P, Brouwers HJH. A study of multiple effects of nano-silica and hybrid fibres on the properties of ultra-high performance fibre reinforced concrete (UHPFRC) incorporating waste bottom ash (WBA). Constr Build Mater. 2014;60:98–110.
- [54] Yu R, Spiesz P, Brouwers HJH. Development of ultra-high performance fibre reinforced concrete (UHPFRC): Towards an efficient utilization of binders and fibres. Constr Build Mater. 2015;75:273–82.
- [55] Bahedh MA, Jaafar MS. Ultra high-performance concrete utilizing fly ash as cement replacement under autoclaving technique. Case Stud Constr Mater. 2018;9:e00202.
- [56] Teng L, Valipour M, Khayat KH. Design and performance of low shrinkage UHPC for thin bonded bridge deck overlay. Cem Concr Compos. 2021;118:103953.

- [57] Liu Y, Wei Y. Effect of calcined bauxite powder or aggregate on the shrinkage properties of UHPC. Cem Concr Compos. 2021;118:103967.
- [58] Zhu Y, Zhang Y, Hussein HH, Liu J, Chen G. Experimental study and theoretical prediction on shrinkage-induced restrained stresses in UHPC-RC composites under normal curing and steam curing. Cem Concr Compos. 2020;110:103602.
- [59] Vigneshwari M, Arunachalam K, Angayarkanni A. Replacement of silica fume with thermally treated rice husk ash in reactive powder concrete. J Clean Prod. 2018;188:264-77.
- [60] Hussain ZA, Aljalawi NMF. Behavior of reactive powder concrete containing recycle glass powder reinforced by steel fiber. J Mech Behav. Mater. 2022;31:233-9.
- [61] Pyo S, Wille K, El-Tawil S, Naaman AE. Strain rate dependent properties of ultra high performance fiber reinforced concrete (UHP-FRC) under tension. Cem Concr Compos. 2015;56:15–24.
- [62] Yang SL, Millard SG, Soutsos MN, Barnett SJ, Le TT. Influence of aggregate and curing regime on the mechanical properties of ultra-high performance fibre reinforced concrete (UHPFRC). Constr Build Mater. 2009;23:2291–8.
- [63] Azmee NM, Shafiq N. Ultra-high performance concrete: From fundamental to applications. Case Stud Constr Mater. 2018;9:e00197.
- [64] Holschemacher K, Weiße D. Economic mix design ultra highstrength concrete. In: Russell HG, editor. Proceedings of the 7th International Symposium on the Utilization of High-Strength/High-Performance Concrete; 2005 Jun 20–24; Washington D.C., USA. ACI, 2005. p. 1133–44.
- [65] ASTM C618-19. Standard Specification for Coal Fly Ash and Raw or Calcined Natural Pozzolan for Use in Concrete. West Conshohocken (PA), USA: ASTM; 2019.
- [66] Hasan M, Saidi T, Muyasir A, Alkhaly YR, Muslimsyah M. Characteristic of calcined diatomaceous earth from Aceh Besar District – Indonesia as cementitious binder. IOP Conf Ser Mater Sci Eng. 2020;933:012008.
- [67] Papadakis VG, Tsimas S. Supplementary cementing materials in concrete Part I: efficiency and design. Cem Concr Res. 2002;32:1525-32.
- [68] Kastis D, Kakali G, Tsivilis S, Stamatakis MG. Properties and hydration of blended cements with calcareous diatomite. Cem Concr Res. 2006;36:1821–26.
- [69] Hamou AT, Petrov N, Luke K. Properties of concrete containing diatomaceous earth. ACI Mater J. 2003;100:73–8.
- [70] Hasan M, Muyasir A, Saidi T, Husaini, Azzahra R. Properties of high strength concrete with calcined diatomaceous earth as cement replacement under compression. Defect Diffus Forum. 2020;402:7–13.
- [71] Hasan M, Riski DDR, Saidi T, Rahman PN. Flexural and splitting tensile strength of high strength concrete with diatomite micro particles as mineral additive. Defect Diffus Forum. 2020;402:50-5.
- [72] Saidi T, Hasan M. The effect of partial replacement of cement with diatomaceous earth (DE) on the compressive strength and absorption of mortar. J King Saud Univ Eng Sci. 2022;34:250–9.
- [73] Funk JE, Dinger DR. Predictive process control of crowded particulate suspensions, applied to ceramic manufacturing. Boston, USA: Kluwer Academic Publishers; 1994.
- [74] Yu R, Spiesz P, Brouwers HJH. Mix design and properties assessment of ultra-high performance fibre reinforced concrete (UHPFRC). Cem Concr Res. 2014;56:29–39.

- [75] Li PP, Cao YYY, Sluijsmans MJC, Brouwers HJH, Yu Q. Synergistic effect of steel fibres and coarse aggregates on impact properties of ultra-high performance fibre reinforced concrete. Cem Concr Compos. 2021;115:103866.
- [76] Saidi T, Hasan M, Riski ADD, Ayunizar RR, Mubarak A. Mix design and properties of reactive powder concrete with diatomaceous earth as cement replacement. IOP Conf Ser Mater Sci Eng. 2020;933:012007.
- [77] Zhou M, Wu Z, Ouyang X, Hu X, Shi C. Mixture design methods for ultra-high-performance concrete - a review. Cem Concr Compos. 2021;124:104242.
- [78] Borges PHR, Fonseca LF, Nunes VA, Panzera TH, Martuscelli CC. Andreasen particle packing method on the development of geopolymer concrete for civil engineering. J Mater Civ Eng. 2014;26:692-7.
- [79] User Guide Elkem Materials Mixture Analyser EMMA, Elkem; 2016.
- [80] Alkhaly YR, Hasan M. Characteristics of reactive powder concrete comprising synthesized rice husk ash and quartzite powder. J Clean Prod. 2022;375:134154.
- [81] Magureanu C, Sosa I, Negrutiu C, Heghes B. Mechanical properties and durability of ultra-high-performance concrete. ACI Mater J. 2012;109(2):177-83.
- [82] ASTM C1437-07. Standard Test Method for Flow of Hydraulic Cement Mortar. West Conshohocken (PA), USA: ASTM International; 2007.

- [83] ASTM C230/230M-08. Standard Specification for Flow Table for Use in Tests of Hydraulic Cement. West Conshohocken (PA), USA: ASTM International; 2008.
- [84] Hasan M, Saidi T. Properties of blended cement paste with diatomite from Aceh Province Indonesia. IOP Conf Ser Mater Sci Eng. 2020;796:012034.
- [85] Haynes H, O'Neill R, Mehta PK. Concrete deterioration from physical attack by salts. Concr Int. 1996;18:63-8.
- [86] Mehta PK. Sulfate attack on concrete: Separating myths from reality. Concr Int. 2000;22(8):57-61.
- QCL Group Technical Note. Sulphate Attack And Chloride Ion Penetration: Their Role In Concrete Durability; 1999.
- [88] Ghazy A, Bassouni MT. Resistance of concrete to different exposures with chloride-based salts. Cem Concr Res. 2017;101:144-58.
- [89] Chindaprasirt P, Homwuttiwong S, Sirivivatnanon V. Influence of fly ash fineness on strength drying shrinkage and sulfate resistance of blended cement mortar. Cem Concr Res. 2004;34:1087-92.
- [90] Chindaprasirt P, Ruzkon S, Sirivivatnanon V. Resistance to chloride peneteration of blended Portland cement mortar containing palm oil fluel ash, rice husk ash and fly ash. Constr Build Mater. 2008;22:932-8.
- [91] Handoo SK, Agarwal S, Agarwal SK. Physicochemical, mineralogical, and morphological characteristics of concrete exposed to elevated temperatures. Cem Concr Res. 2002;32:1009-18.